

Coastal dune modelling from airborne LiDAR, terrestrial LiDAR and Structure from Motion–Multi View Stereo

Carlos H. Grohmann^{1*}, Guilherme P.B. Garcia², Alynne A. Affonso¹, Rafael W. Albuquerque¹

(1) Institute of Energy and Environment, University of São Paulo, São Paulo, Brazil

(2) Institute of Geosciences, University of São Paulo, São Paulo, Brazil

all authors: Spatial Analysis and Modelling Lab (SPAMLab, IEE-USP)

* corresponding author: guano@usp.br

Abstract—In this work, we present an analysis of the Garopaba dune field, southern Brazil, based on data from Airborne LiDAR (ALS - surveyed in 2010), Terrestrial LiDAR (TLS - surveyed in 2019) and Structure from Motion–Multi View Stereo (SfM-MVS - surveyed in 2019). Although sand dunes are commonly regarded as a challenge to traditional photogrammetry due their homogeneous texture and spectral response, in this research image matching was successful in all areas of the survey due the presence of superficial features (footprints and sandboard tracks) and visibility of the sedimentary stratification, highlighted by heavy minerals. The SfM-MVS DEM accuracy was evaluated by comparison with a TLS DEM, resulting in RMSE of 0.08m and MAE of 0.06m. Displacement of dune crest lines from the ALS and SfM-MVS DEMs resulted in a migration rate of ≈ 5 m/year between 2010 and 2019, in good agreement with rates derived from satellite images and historical aerial photographs of the same area. SfM-MVS is a low-cost solution with fast and reliable results for 3D modelling and continuous monitoring of coastal dunes.

I. INTRODUCTION

To better understand the dynamic environments in which aeolian dune fields occur, repeated topographic surveys of the landscape are needed [1]. As the sand supply of dune fields is sensitive to patterns of wind and rainfall, changes in dune field volume and morphology can be related to climate change [2].

Digital Elevation Models (DEMs) of aeolian dunes can be constructed by several methods such as traditional field techniques (levelling, Total Station), interpolation of contour lines or Differential/Real-time kinematic (RTK) GPS points, LiDAR (Light Detection and Ranging) surveys, either airborne (ALS – Airborne Laser Scanner) or terrestrial (TLS – Terrestrial Laser Scanner) and, more recently, Structure from Motion–Multi View Stereo (SfM-MVS) [3-5]. Remotely Piloted Aircrafts

(RPAs) have been used as platform for SfM-MVS image collection and for lightweight LiDAR systems [6].

In this work, we present an analysis of the Garopaba dune field, southern Brazil, based on DEMs from ALS (surveyed in 2010), TLS and SfM-MVS (both surveyed in 2019). Altimetric accuracy of the SfM-MVS DEM was validated by comparison with TLS data collected during the same fieldwork campaign of the RPA flights. The use of SfM-MVS for aeolian dunes modelling is recommended and the factors that contributed to a successful 3D reconstruction are discussed.

II. METHODS

The Garopaba dune field, located in southern Brazil, is composed of unvegetated and vegetated aeolian dunes. The unvegetated dunes are represented by mostly barchanoid chains, while the vegetated ones include parabolic dunes, blowouts and foredunes [7] (Fig. 1).

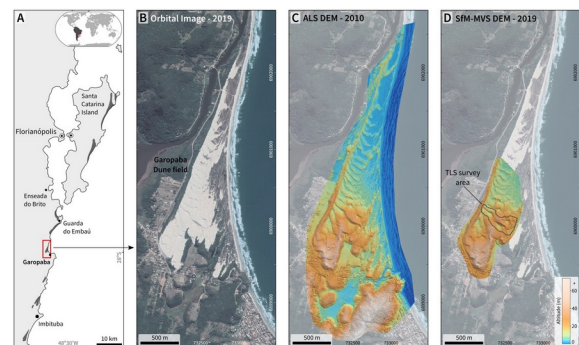


Figure 1. A) Location of study area in southern Brazil; B) Satellite image of the Garopaba dune field (image date: 07-30-2017); C) ALS DEM (2010); D) SfM-MVS DEM (2019), with TLS survey area shown. Elevation colour scale is the same for C and D. Shaded relief illumination: N25°, 30° above horizon.

ALS data were collected on October 2010 by Geoid Laser Mapping Co. using an Optech ALTM 3100 sensor with a saw-tooth scanning pattern, density of about 4 points/m², measured from an altitude of ≈1,200m (≈4,000ft). Raw LiDAR data (with up to four laser pulses) were processed by Geoid and delivered with vertical accuracy of 0.15m (1σ) and horizontal accuracy of 0.5 m (1σ). ALS first returns were imported into GRASS-GIS as vector points and interpolated with bilinear splines to create a DEM with 0.5m spatial resolution (Fig. 1C).

TLS data (110 point clouds) were collected with a FARO Laser Scanner Focus^{3D} S120. To overcome the heterogeneous distribution of data common to TLS, with a very high density of points near the scanner, the full point cloud was subsampled in FARO Scene with a minimum distance filter of 2cm between points. This point cloud was gridded to a raster in GRASS-GIS using the mean elevation value of LiDAR points within 10cm cells (r.in.xyz module). To fill empty (null) cells, the raster was converted to vector and a DEM with 10cm spatial resolution was created by interpolation with bilinear splines (Fig. 4A).

Images for the SfM-MVS reconstruction were acquired by a DJI Phantom 4 Pro RPA (1" CMOS 20MP sensor, global shutter). Flight missions were executed with height above takeoff point of 100m (pixel size ≈2.7cm) and 75% overlap along and across-track. Six missions were flown, covering an area of ≈869,000m² with 810 images. Weather conditions during fieldwork were of dark skies with light rains scattered throughout the day. The SfM-MVS workflow was processed in Agisoft Metashape Pro version 1.5.14. In the SfM step, images were aligned with ‘High’ accuracy; the MVS reconstruction was set to ‘High’ quality and ‘aggressive’ depth filtering. The full SfM-MVS point cloud was subsampled (thinned) with LAsTools by extracting every 125th point, imported into GRASS-GIS as vector points and interpolated with bilinear splines to a DEM with 0.5m resolution. The thinning value was determined after experimentation, and the goal was to obtain a similar number of points, within the interpolation area, for the ALS and SfM point clouds (Table 1).

TABLE I. OVERVIEW OF DATASETS USED IN THIS STUDY

Dataset	DEM Area (m ²)	# points	points/m ²
ALS (full)	4,434,722	11,574,555	2.6
ALS (SfM area)	740,922	2,380,005	3.2
SfM-MVS (full)	740,922	344,595,132	465.1
SfM-MVS (thin 125 th pt)	740,922	2,376,632	3.2
SfM-MVS (TLS area)	80,413	28,158,102	350.1
SfM-MVS (10 cm grid)	80,413	8,039,750	99.9
TLS (full)	80,413	1,187,708,492	14770.1
TLS (2 cm filter)	80,413	170,141,709	2115.8
TLS (10 cm grid)	80,413	7,028,118	87.4

The point cloud datasets are available via the OpenTopography Facility. The following datasets were used in this study: OpenTopography ID [OT.032013.32722.1](#) (ALS), [OTDS.072019.32722.1](#) (SfM), [OTDS.102019.32722.1](#) (TLS).

III. RESULTS

The DEMs produced from the TLS (Fig. 2A) and SfM-MVS (Fig. 2B) are very similar, without any major difference in elevation or in the reconstruction of topographic features. Upon a closer inspection, the SfM-MVS DEM presents a small scale surface roughness not visible in the TLS DEM. To visually evaluate this difference, surface roughness of the DEMs was calculated as the standard deviation of slope [8] in a 5x5 pixels neighbourhood (0.5x0.5 m).

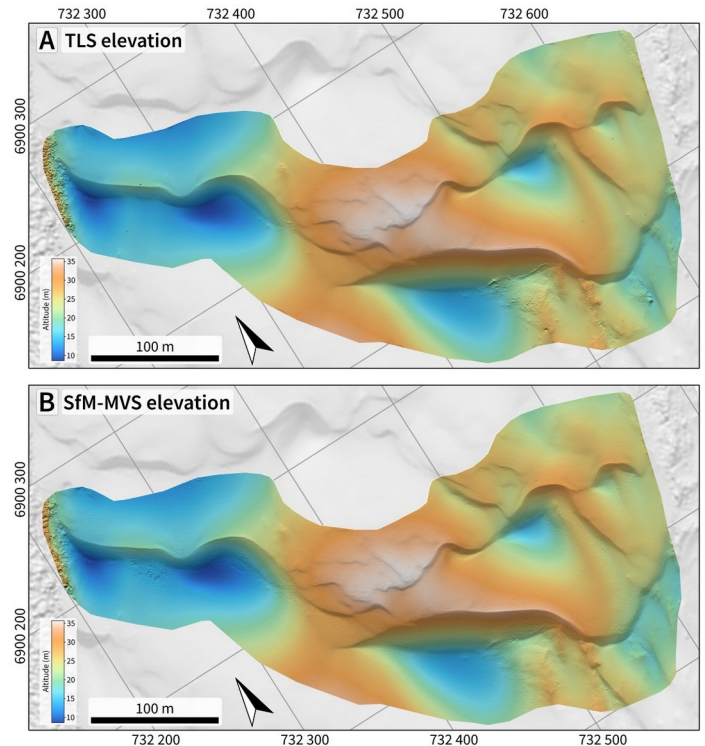


Figure 2. A) TLS DEM; B) SfM-MVS DEM. Elevation colour scale is the same for A and B. Shaded relief illumination: N25°, 30° above horizon.

The TLS DEM has a smooth surface, with higher roughness values on vegetated areas and over some of the places where the TLS equipment was positioned (Fig. 3A). These spots can be related to a small mismatch between adjacent scans, where in one there is no data (under the scanner), so the gridding procedure cannot compensate the difference and the result is a small circular patch of the terrain slightly above or below its surroundings. Dune crests are well marked by above-average roughness. Footprints and track marks are also visible, with lower roughness values. The SfM-MVS DEM shows a widespread distribution of low and average roughness values (Fig. 3B). While the dune crests can be identified, track marks are no longer visible and the patch of vegetation near the sandboard tracks cannot be discriminated based on its roughness. A set of footprints seen in the central-eastern portion of the TLS roughness map is not visible in the SfM-MVS roughness because the SfM-MVS survey was carried out before the TLS survey could cover that area.

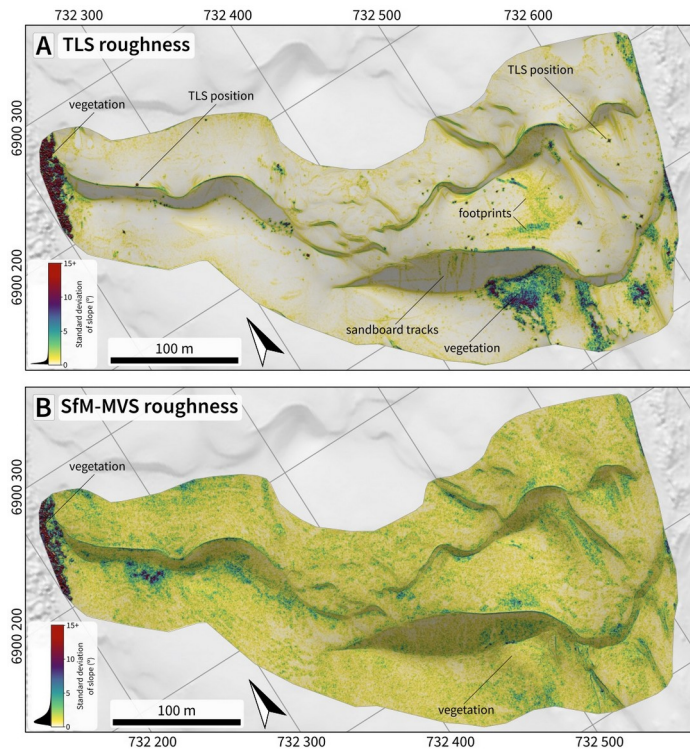


Figure 3. Surface roughness maps, calculated as the standard deviation of slope in a 5x5 window: A) TLS; B) SfM-MVS. Roughness colour scale is the same for A and B.

The vertical accuracy of the SfM-MVS DEM was calculated from a set of 2,000 random points, resulting in RMSE of 0.08m and MAE of 0.06m.

Besides a good correlation to the TLS DEM, the full SfM-MVS DEM (Fig. 4B) shows a good fit with elements of the landscape that didn't experienced significant change between the surveys, such as the road bordering the dune field to west and southwest (in grey in Fig. 4C, indicating no elevation difference).

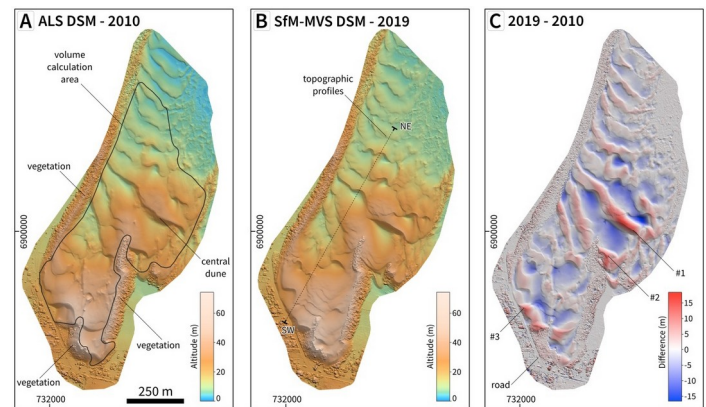


Figure 4. A) ALS DEM (2010), with volume calculation area polygon; B) SfM-MVS DEM (2019), with topographic profiles location; C) DEM of differences (2019-2010). Numbers in C are discussed in the text.

Some notable differences are indicated as #1, #2 and #3 in Fig. 4C: #1 marks the highest positive difference (where the SfM-MVS surface is above the ALS), related to the migration of a large 'central dune' with accumulation of sand towards a vegetated ridge in #2; #3 shows the migration of the dune field over the road. In this place, the town hall needs to remove the sand periodically to keep the road open.

The polygon for volume calculation encloses only unvegetated areas in both surveys (see Fig. 4A). Using the ALS and SfM DEMs with 0.5 m resolution, the calculated sand volumes were 9,035,115.45 m³ for 2010 and 9,010,844.95 m³ for 2019 (a decrease of 24,270.50 m³ or 0.2%).

Dune crest displacement lines drawn over the DEMs (Fig. 5) yielded a mean azimuth of 215.5° and mean length of ≈44.5m (mean: 44.3m, median: 44.7m). A mean length of 44.5m in 9 years corresponds to a dune migration rate of ≈5 m/year. We consider these rates to be in agreement with rates of 6-7 m/year derived from interpretation of historical aerial photographs and satellite images with coarser spatial resolution [9].

Topographic profiles (Fig. 6) illustrate dune movement from 2010 to 2019, with migration of the lee side and relatively less change over the stoss side of large compound dunes.

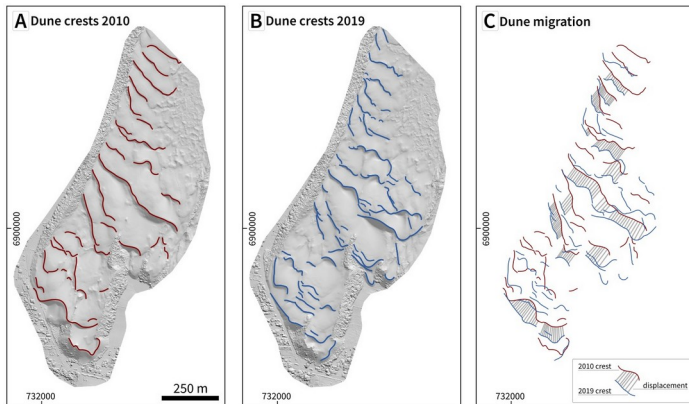


Figure 5. Determination of dune migration between 2010 and 2019 surveys. A) dune crests of 2010, over shaded relief image of ALS DEM; B) dune crests of 2019, over shaded relief image of SfM-MVS DEM; C) displacement lines (grey) connecting crest lines.

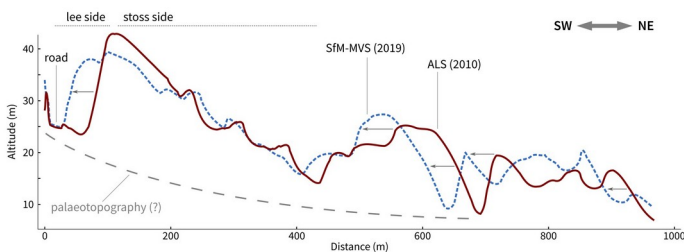


Figure 6. Topographic profiles across the dune field (location in Fig. 4B.)

IV. DISCUSSION

Although sand dunes are commonly regarded as a challenge to traditional photogrammetry due their homogeneous texture and spectral response, yielding poor results in image matching, the presence of superficial features (footprints and sandboard tracks) and visibility of the sedimentary stratification highlighted by heavy minerals, allowed a successful SfM-MVS reconstruction.

ALS might be acquired in little time, but it is by far the most expensive, imposing a serious constraint on repeated surveys, especially for researchers in developing countries or without access to state-funded coastal monitoring programs.

TLS has an intermediate cost of acquisition (since the equipment can be rented and operated by the research team) but it demands more fieldwork and more processing time. In our case we needed three days for the TLS survey and around three weeks of full-time work to produce a DEM of $\approx 80,400\text{m}^2$.

We were able to cover $\approx 740,900\text{m}^2$ with six RPA missions in under three hours. Processing time in a medium-range workstation (i.e., i7 processor, dedicated GPU) was ≈ 13 hours.

SfM-MVS is a low-cost solution capable of delivering fast and reliable results for 3D modelling and continuous monitoring of coastal dunes.

ACKNOWLEDGMENT

We would like to thank the financial support of FAPESP (grants #2009/17675-5, #2016/06628-0) and CNPq (grants #423481/2018-5, #304413/2018-6). This study was financed in part by CAPES Brasil – Finance Code 001 through PhD scholarships to G.P.B.G, A.A.A. and R.W.A. This work acknowledges the services provided by the OpenTopography Facility with support from the National Science Foundation under NSF Award Numbers 1557484, 1557319, and 1557330.

REFERENCES

- [1] Conlin, M., Cohn, N., Ruggiero, P., 2018. A Quantitative Comparison of Low-Cost Structure from Motion (SfM) Data Collection Platforms on Beaches and Dunes. *Journal of Coastal Research* 34 (6), 1341–1357.
- [2] Gaylord, D. R., Foit, F. F., Schatz, J. K., Coleman, A. J., 2001. Smith Canyon dune field, Washington, U.S.A: relation to glacial outburst floods, the Mazama eruption, and Holocene paleoclimate. *Journal of Arid Environments* 47 (4), 403 – 424.
- [3] Mitasova, H., Overton, M., Harman, R. S., 2005. Geospatial analysis of a coastal sand dune field evolution: Jockey’s Ridge, North Carolina. *Geomorphology* 72, 204–221.
- [4] Gonçalves, J., Henriques, R., 2015. UAV photogrammetry for topographic monitoring of coastal areas. *ISPRS Journal of Photogrammetry and Remote Sensing* 104, 101 – 111.
- [5] Guisado-Pintado, E., Jackson, D., Rogers, D., 2019. 3D mapping efficacy of a drone and terrestrial laser scanner over a temperate beach-dune zone. *Geomorphology* 328, 157–172.
- [6] Solazzo, D., Sankey, J.B., Sankey, T.T. and Munson, S.M., 2018. Mapping and measuring aeolian sand dunes with photogrammetry and LiDAR from unmanned aerial vehicles (UAV) and multispectral satellite imagery on the Paria Plateau, AZ, USA. *Geomorphology*, 319, 174-185.
- [7] Martinho, C. T., Giannini, P. C. F., Sawakuchi, A. O., Hesp, P. A., 2006. Morphological and depositional facies of transgressive dunefields in the Imbituba-Jaguaruna region, Santa Catarina State. *Journal of Coastal Research* SI39, 143–168.
- [8] Grohmann, C. H., Smith, M. J., Riccomini, C., 2010. Multiscale Analysis of Topographic Surface Roughness in the Midland Valley, Scotland. *Geoscience and Remote Sensing, IEEE Transactions on* 49 (4), 1200–1213.
- [9] Mendes, V. R., Giannini, P. C. F., Guedes, C. C. F., DeWitt, R., de Abreu Andrade, H. A., 08 2015. Central Santa Catarina coastal dunefields chronology and their relation to relative sea level and climatic changes. *Brazilian Journal of Geology* 45, 79 – 95.